Alterations in Chromatin Conformation Are Accompanied by Reorganization of Nonchromatin Domains That Contain U-snRNP Protein p28 and Nuclear Protein p107

HAROLD C. SMITH,* DAVID L. SPECTOR,* CHRISTOPHER L. F. WOODCOCK,‡ ROBERT L. OCHS,* and JASWANT BHORJEE§

Department of Pharmacology, Baylor College of Medicine, Houston, Texas 77030; ‡Department of Zoology, Morrill Science Center, University of Massachusetts 01003; and §Division of BioMedical Sciences, Meharry Medical College, Nashville, Tennessee 37208.

ABSTRACT The intranuclear distribution of nuclear matrix-associated protein p107 and the 28-kD Sm antigen of U-snRNPs have been studied using double-label immunofluorescence and immunoperoxidase electron microscopy. In interphase nuclei of HeLa cells, Novikoff hepatoma cells, and rat kangaroo kidney cells, p107 was confined to discrete interchromatin domains. These domains had an irregular contour, with an average diameter of 1–1.5 μm. Each domain appeared to be composed of interconnected granules. The Sm antigen co-localized and appeared concentrated in these domains but also showed some general nucleoplasmic distribution. During mitosis, the interchromatin domains disassembled such that the Sm portion redistributed to the perichromosomal and spindle regions and the p107 component redistributed throughout the mitotic cytoplasm. During anaphase, p107 assembled into discrete clusters throughout the mitotic cytoplasm. The Sm antigen was not a component of these clusters. Double-label immunofluorescence with anti-p107 and the anti-DNA tight-binding protein, $AhNa_1$, showed that the extranuclear p107 domains assumed an interchromatin localization only after the chromosomes had decondensed. The correlation between chromosome decondensation and the occurrence of p107 within interchromatin domains was also observed during chicken erythrocyte nuclear reactivation. We propose that the discrete interchromatin domains that contain p107 and p28 may be important for processing and splicing of RNA and that their structural assembly within nuclei is sensitive to the presence of the transcriptionally active conformation of chromatin.

Ribonucleoprotein particles (RNPs)[1] and the RNP network make up a significant portion of the nucleoplasm (3, 5–7, 15, 41). A network of peri- and interchromatin fibers and granules extends throughout the interior of the nucleus to form a continuum from the nucleolus to the nuclear envelope and pore complexes (5). The perichromatin fibrils are believed to be the first site where nascent heterogeneous nuclear RNA (hnRNA) appears (13, 17, 18, 39, 42). Soon afterwards, nascent transcripts can be localized within the interchromatin regions where the mechanisms for mRNA maturation and transport to the cytoplasm have been proposed to reside (3, 15–18, 42, 43).

The 1–2-M salt-resistant RNA protein components of the RNP network prepared from hnRNPs (19, 20, 23, 40, 52) or whole nuclei (4, 11, 31, 32, 34–38, 44, 51, 53) are enriched in specific high molecular weight proteins and hnRNA nascent transcripts, and contain many of the U-small nuclear RNAs (snRNAs). These findings have led several investigators to propose that salt-resistant RNP complexes may be important for the packaging, posttranscriptional modification, and transport of mRNA (for review see reference 5).

[1] Abbreviations used in this paper: CRLM, polyclonal IgG reactive with p107; hnRNA, heterogeneous nuclear RNA; hnRNPs, ribonucleoprotein particles containing hnRNA; RNPs, ribonucleoprotein particles; Sm, monoclonal IgG reactive with U snRNPs; snRNA, small nuclear RNAs; snRNPs, RNPs containing snRNA.

THE JOURNAL OF CELL BIOLOGY · VOLUME 101 AUGUST 1985 560-567

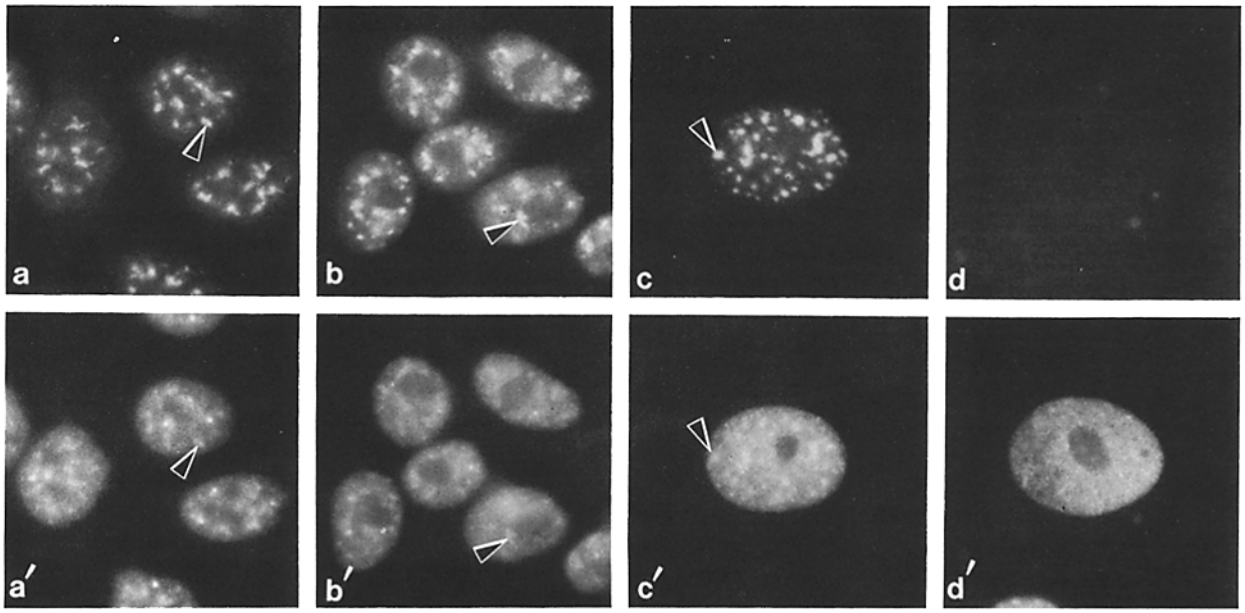

FIGURE 1 Double-label immunofluorescence of various cultured cells with CRLM and Sm. HeLa S_3 cells, Novikoff rat hepatoma cells, rat kangaroo kidney (PtK-2) cells, and *Xenopus* kidney (A_6) cells were cultured as described in Materials and Methods, simultaneously reacted with CRLM and Sm, followed by second antibody (see Materials and Methods). *a* and *a′*, *b* and *b′*, *c* and *c′*, and *d* and *d′* correspond to CRLM and Sm fluorescence micrographs of HeLa S_3 cells, Novikoff hepatoma cells, PtK-2 cells, and A_6 cells, respectively. Arrowheads indicate areas of identical labeling. ×1,000.

In this study, we have used two antibodies that react with components of the salt-resistant RNP complexes: Sm, which is a monoclonal IgG reactive with the 28-kD protein (p28) in U1, U2, U4, U5, and U6 snRNPs (RNP particles containing snRNA) (28, 32, 50, 54); and CRLM, a polyclonal IgG reactive with a 107-kD nuclear protein (p107) (47, 49).[2] Both antibodies were used to examine the in situ morphology and intracellular distribution of RNP complexes during mitosis and under conditions where chromatin condensation was experimentally altered. We show that there is a correlation between the condensation state and/or the transcriptional activity of chromatin, and the morphology and assembly of the interchromatin domains that contain RNP complexes.

MATERIALS AND METHODS

Source of Antibodies: Chicken polyclonal IgG reactive with a 107-kD protein (pI = 8.7–8.8) (47, 49)[2] was obtained by immunizing mature laying hens with whole rat liver nuclear matrices (5, 46) in complete Freund's adjuvant, 500 μg protein per immunization period. Hens were immunized by intradermal, subcutaneous, and intramuscular injection once each week for 4 wk, rested for 2 wk, immunized on the sixth week using incomplete Freund's adjuvant, and bled on the seventh week. IgG was precipitated from serum with phosphate-buffered 34% sodium sulfate, reprecipitated with 15% sodium sulfate, and stored in phosphate-buffered saline (PBS) at −20°C. This IgG was designated CRLM.

Hybridoma cells secreting the monoclonal antibody (Sm) (28) were a gift from Dr. Joan A. Steitz to Dr. D. L. Spector. IgG was prepared from hybridoma supernatant by precipitation with 18% ammonium sulfate. Sm IgG immunoprecipitated U1, U2, U4, U5, and U6 snRNAs (28) and specifically identified a 28-kD protein on immunoblots (47, 49).[2] No snRNAs could be immunoprecipitated by CRLM (unpublished results).

Monoclonal antibody ($AhNa_1$) against a 55-kD DNA tight-binding protein was obtained as previously described (8, 55).

Preparation of Cells and Immunocytochemistry: Rat kangaroo kidney cells (PtK-2), rat hepatocyte cells (clone 9), HeLa S_3 cells (American Type Culture Collection, Rockville, MD), and Novikoff hepatoma cells (obtained from ascites fluid) were grown in Dulbecco's modified Eagle's medium (Gibco Laboratories, Grand Island, NY) with 5–10% fetal calf serum. *Xenopus* kidney cells (A_6) (American Type Culture Collection) were grown in RPMI-1640 medium (Gibco Laboratories) containing 10% fetal calf serum. The cells were fixed with 2% paraformaldehyde in PBS (15 min, 4°C) and permeabilized with 0.4% Triton X-100 in PBS (15 min, 4°C). Prepared cells were reacted with CRLM, at 1:200 dilution or double-labeled by the simultaneous addition of CRLM with Sm (1:5 dilution) or $AhNa_1$ (1:50 dilution). After a 1-h incubation at 37°C and subsequent washes, fluorescein-conjugated goat anti-chicken IgG and rhodamine-conjugated goat anti-human or anti-mouse IgG (Cappel Laboratories, Cochranville, PA) were added as second antibody. After washes, slides were mounted with PBS that contained 90% glycerol and 4% *n*-propylgallate, and were examined on a Zeiss fluorescence microscope equipped with a Nikon FX-35A camera and Microflex UFX photometer.

Enucleation and Fusion of Mouse L-929 Cells with Chicken Erythrocyte Nuclei: Mouse L-929 cells were enucleated by incubation in media that contained 10 μg/ml cytochalasin B (Aldrich Chemical Co., Milwaukee, WI) for 20 min, followed by centrifugation (12,000 *g*, 45 min) as previously described (27). Cytoplasts were incubated for 5 min at 4°C in Earle's balanced salt solution that contained UV-inactivated Sendai virus (200 haemagglutination U/ml). Treated cytoplasts were then overlaid with a suspension of 14–18-d chick embryo erythrocytes (10^8 per dish) for 15 min at 4°C followed by 60 min at 37°C. Unfused erythrocyte nuclei were removed by washing and the hybrid cells were incubated in fresh medium for 16 h before preparation for immunocytochemistry. For the production of heterokaryons, the enucleation step was omitted.

Immunoelectron Microscopy: Cells were fixed in 1% glutaraldehyde in PBS (pH 7.3) for 15 min at room temperature. Fixed cells were then washed three times for 15 min each in 0.5 mg/ml sodium borohydride and incubated in 0.2% Triton X-100/0.5% normal goat serum in PBS for 5 min at 4°C. Samples were then washed for 30 min in several changes of PBS that contained 0.5% normal goat serum and incubated in the appropriate primary antibody (Sm or CRLM) at a dilution of 1:5 or 1:100, respectively, for 1 h at 37°C, and further washed overnight in PBS at 4°C to remove unbound antibody. Samples were then incubated in peroxidase-conjugated second antibody (Cappel Laboratories) at a dilution of 1:20 for 1 h at 37°C, and subsequently washed in PBS for 15 min and then in 0.05 M Tris-HCl (pH 7.6) for 30 min at 4°C. Samples were then incubated in 0.05% 3,3′-diaminobenzidine in 0.05 M Tris-HCl (pH 7.6) for 25 min at room temperature and then suspended in 0.05% 3,3′-diaminobenzidine supplemented with 0.01% H_2O_2 for 4 min, washed in 0.05 M Tris-HCl (pH 7.6) for 30 min, and fixed in 2% OsO_4 in 0.1 M sodium cacodylate buffer (pH 7.3) for 1 h. Subsequently, the samples were rinsed in distilled water, dehydrated in a graded series of ethanol followed by 100% propylene oxide, and infiltrated and embedded in Poly/Bed 812 (Polysciences, Inc., Warrington, PA). Polymerization was carried out at 60°C for 48 h.

[2] Smith, H. C., R. L. Ochs, E. A. Fernandez, and D. L. Spector, manuscript in preparation.

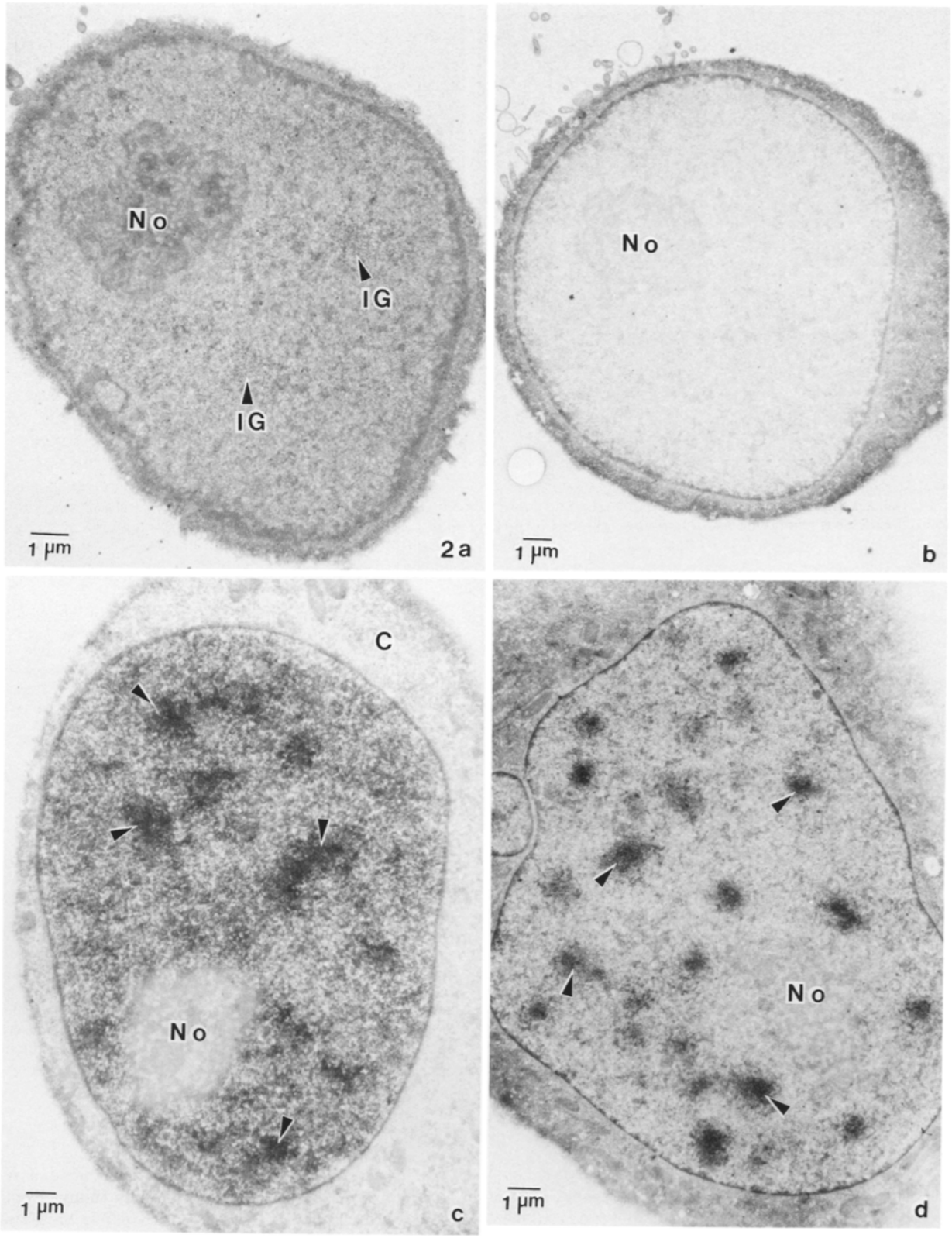

FIGURE 2 Immunoperoxidase electron microscopy of Sm and CRLM reactivity. (*a*) PtK2 cells fixed (glutaraldehyde, osmium tetroxide) and stained (uranyl acetate, lead citrate) for electron microscopy by standard procedures show little differentiation within the nucleoplasm. Aside from the nucleolus (*No*) and several patches of interchromatin granules (*IG*), no specific nuclear domains are revealed. (*b*) PtK2 cells immunoreacted with pre-immune chicken serum as a primary antibody followed by peroxidase-conjugated second antibody (without poststaining) exhibit no immunostaining. (*c*) PtK2 cells reacted with the Sm antibody (without poststaining) exhibit a reticular nuclear staining pattern (arrowheads) as well as diffuse nuclear immunostaining. Both the nucleolus (*No*) and the cytoplasm (*C*) are negative. No poststaining. (*d*) PtK2 cells immunostained with the CRLM antibody (without poststaining) exhibit the same type of staining (arrowheads) as with the Sm antibody; however, the diffuse nuclear staining is not present after CRLM immunostaining.

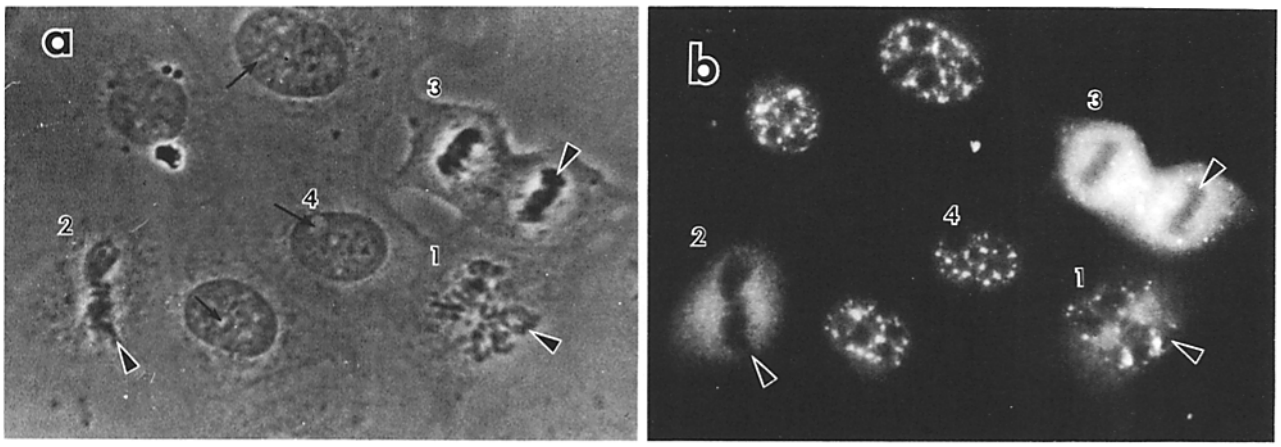

FIGURE 3 Interphase and mitotic distribution of CRLM antigens. Cultured hepatocytes were prepared for immunocytochemical analysis, reacted with CRLM and fluorescein second antibody as described in Materials and Methods. *a* and *b* are phase-contrast and fluorescence micrographs, respectively. Prophase, metaphase, anaphase, and interphase are labeled 1-4, respectively. Arrowheads point to the position of the chromosomes. Arrows point to nucleoli. ×1,000.

Selected cells were sectioned on an LKB Nova ultramicrotome (LKB Instruments, Inc., Gaithersburg, MD) using a DuPont diamond knife (DuPont Co., Wilmington, DE). Sectons were examined without poststaining in a JEOL 100C transmission electron microscope operated at 60 kV.

RESULTS

Co-localization of the Sm and CRLM Antigens by Whole Cell Immunocytochemistry

CRLM and Sm immunoreactivity was observed in a variety of cell types (Fig. 1). Double-immunolabeling with CRLM and Sm resulted in similar but not identical immunofluorescence in HeLa S_3 cells (Fig. 1, *a* and *a'*), Novikoff hepatoma cells (Fig. 1, *b* and *b'*), and PtK-2 cells (Fig. 1, *c* and *c'*). CRLM and Sm immunofluorescent speckles co-localized and were identical in size, shape, and number; however, unlike CRLM, Sm antibody also produced general nucleoplasmic fluorescence. These results demonstrate that the CRLM antigen is a component of discrete interchromatin domains common to those that contain the Sm antigen. Interestingly, Sm was immunoreactive in *Xenopus* kidney cells whereas CRLM was not (Fig. 1, *d* and *d'*). These findings demonstrate that the Sm and CRLM antigens are distinct and suggest that these two proteins may have different evolutionary patterns.

Immunoelectron Microscopy of the Interchromatin Domains

Under standard electron microscopic staining conditions (see Materials and Methods), PtK-2 nucleoplasm shows less definition of heterochromatic and RNP network regions than that observed in other cells. However, the nucleolus, fibrous lamina, and regions of interchromatin granules can be seen (Fig. 2*a*). Immunoperoxidase staining (see Materials and Methods) showed that the Sm antigen, p28, was concentrated within clusters (Fig. 2*c*), but that it also had a general nucleoplasmic distribution. These results are similar to those in Fig. 1, and in addition, suggest that many of the Sm clusters are interconnected to form a reticulum. Discrete dense clusters of CRLM immunoreactivity (Fig. 2*d*) similar to those in Fig. 1 were also observed. Unlike p28, p107 was confined to these discrete patches.

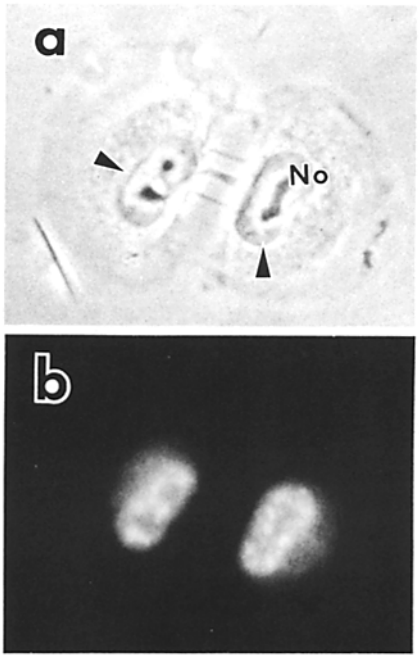

FIGURE 4 Intranuclear CRLM domains in late telophase. Preparation of cultured hepatocytes and immunocytochemistry was as in Fig. 3. *a* and *b* are phase-contrast and fluorescence micrographs, respectively. Arrowhead points to distinct nuclear envelope. *No*, nucleolus. ×1,000.

Mitotic Distribution of p107 in Hepatocytes

Subconfluent cultured hepatocytes, examined 3 h after feeding, were enriched in metaphase cells. In any given field, cells at various stages of mitosis were readily observed (Fig. 3). In prophase, the CRLM speckles were no longer regularly distributed throughout the nucleoplasm but instead appeared clustered close to the chromosomal arms. The chromosomes were not immunoreactive. By the metaphase plate stage, CRLM reactivity appeared as a diffuse haze of immunoreactivity completely surrounding the chromosome mass but excluded from it. The metaphase plate stage showed the weakest CRLM reactivity of the cell cycle. The strongest CRLM reactivity was seen during anaphase. Though the chromo-

somes remained negative, brilliant speckles appeared in the mitotic cytoplasm which were immersed in a bright haze of reactivity. During late telophase, CRLM speckles localized within daughter nuclei (Fig. 4). At this time, the nuclear contents were clearly delimited by a distinct nuclear envelope and nucleoli were apparent.

Relationship of p107 Domain Morphology to Chromatin Condensation State during Mitosis

From the above results, it appeared that the structural assembly of p107-containing domains was influenced by factors and/or events related to chromatin condensation states. This relationship was more carefully evaluated in double-label experiments with CRLM and the monoclonal antibody, $AhNa_1$, which reacts with a 55-kD DNA tight-binding chromatin protein (8, 55). This allowed us to coordinately follow the fate of chromatin and p107.

During the metaphase plate stage when CRLM appeared as a weak haze, $AhNa_1$ reacted only with the chromosomes (Fig. 5, *a–c*, and reference 8). As in the preceding experiments (Fig. 3), CRLM fluorescence intensity increased and appeared as a bright haze with brilliant discrete speckles in early anaphase (Fig 5, *d* and *e*). $AhNa_1$ showed dense reactivity with the chromosomes during anaphase (Fig. 5*f*) and began to assume its very fine speckling pattern of the interphase nucleoplasm in mid telophase (Fig. 5, *g* and *i*). However, the dense fluorescence of $AhNa_1$ at this time compared to that of interphase showed that most of the chromosomes were still condensed (Fig. 5). The intranuclear localization of p107 therefore appears to be a late event which follows chromatin decondensation in late telophase.

Differential Mitotic Distribution of p28 and p107

Though the 28-KD Sm antigen co-localized with p107 in interphase, its mitotic distribution was markedly different (Fig. 6). In prophase, p28 localized homogeneously between the condensing chromosomes and was not concentrated within speckles (Fig. 6*b*), whereas p107 remained within the speckles (Fig. 6*c*). Again, PtK-2 chromosomes showed no immunoreactivity with either Sm or CRLM antibodies throughout mitosis. In metaphase and early anaphase, p28 appeared localized within a "cloud" in the spindle and perichromosomal regions (Fig. 6, *e* and *h*). Interestingly, the "Sm cloud" appeared to remain stationary during anaphase chromosome segregation (Fig. 6*h*). As in Fig. 3, CRLM was dispersed throughout the metaphase and anaphase cell and began to reassemble as extranuclear domains during anaphase (Fig. 6, *f* and *i*). The telophase distribution of p28 was similar to that of prophase in its homogeneous localization between the condensing chromosomes (Fig. 6*k*). At this time, p107 speckles were still extranuclear though their number had increased five- to sixfold (compare Fig. 6, *i* and *l*). Therefore,

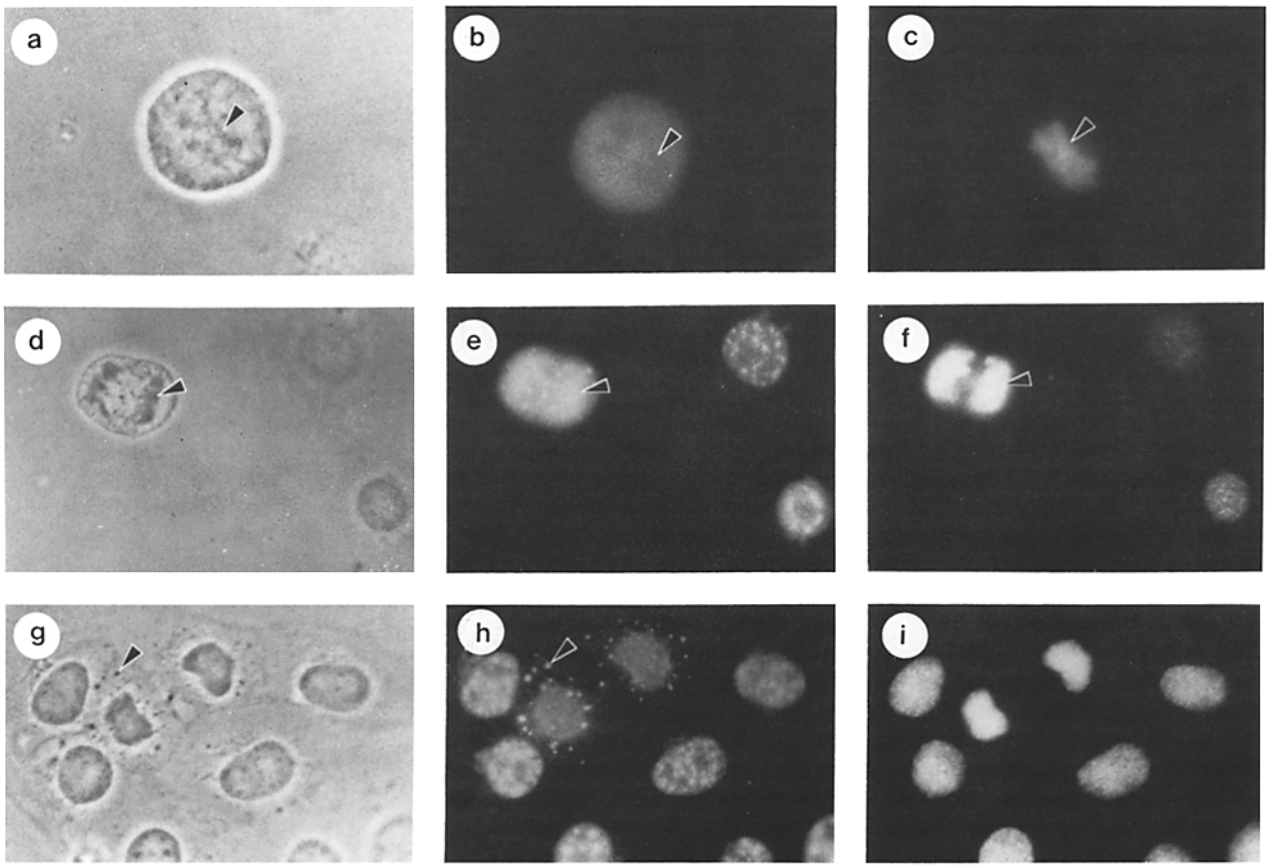

FIGURE 5 Double-label immunofluorescence of clone 9 mitotic cells with CRLM and $AhNa_1$. Cultured hepatocytes were prepared and reacted simultaneously with $AhNa_1$ and CRLM followed by fluorochrome-conjugated second antibody as described in Materials and Methods. (*a–c*) Phase-contrast and CRLM and $AhNa_1$ fluorescence, respectively, of a metaphase cell. Arrowheads point to the chromosomes. (*d–f*) Phase-contrast and CRLM and $AhNa_1$ fluorescence, respectively, of an anaphase cell. Arrowheads point to the chromosomes. (*g–i*) Phase-contrast and CRLM and $AhNa_1$ fluorescence, respectively, of a telophase cell. Arrowheads point to CRLM clusters. ×1,000.

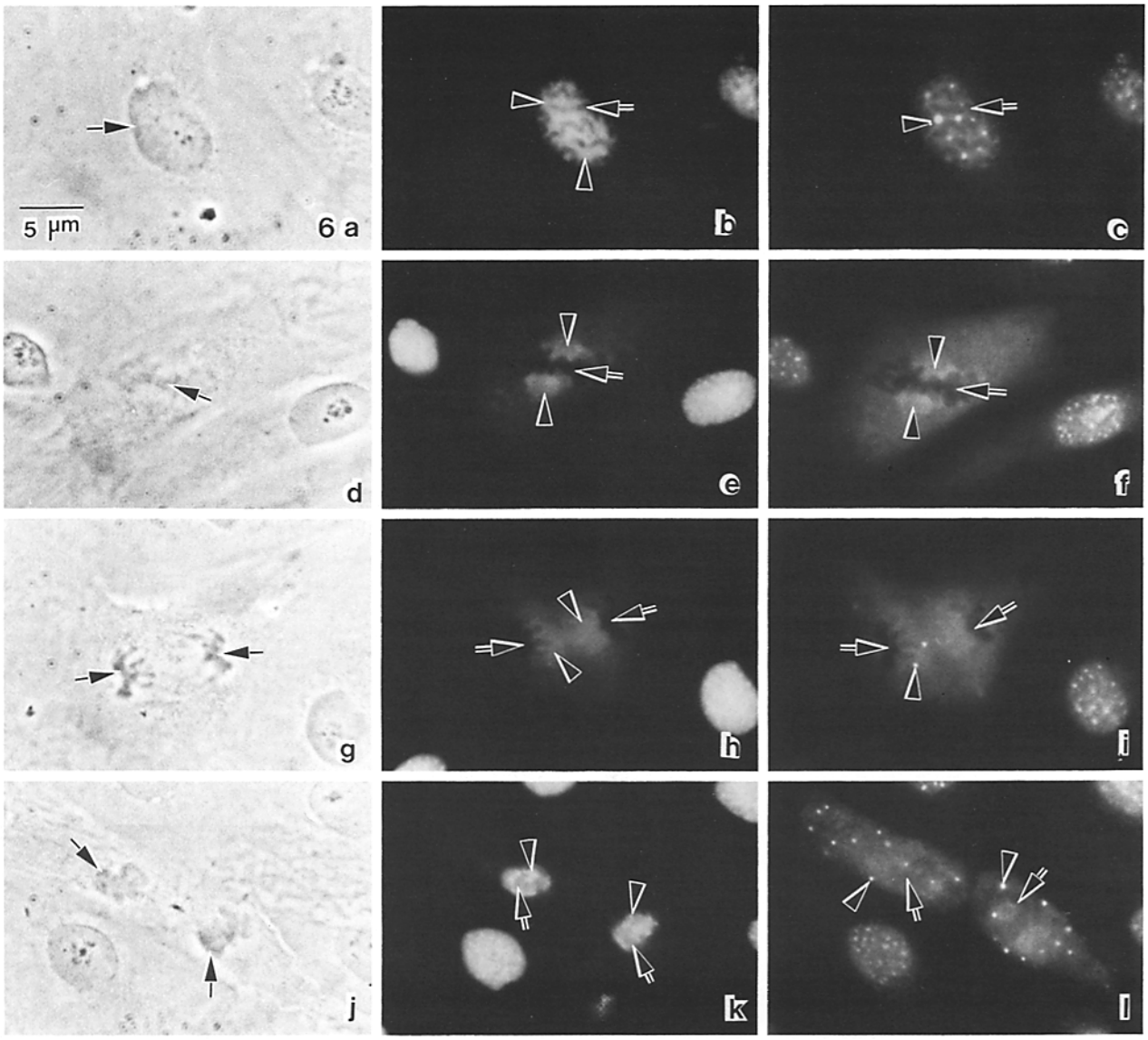

FIGURE 6 Double-label immunofluorescence of mitotic PtK-2 cells with Sm and CRLM. PtK-2 cells were prepared and simultaneously reacted with Sm and CRLM followed by fluorochrome-conjugated second antibody. (*a–c*) Prophase; (*d–f*) metaphase; (*g–i*) anaphase; and (*j–l*) telophase. (*a,d,g,* and *j*) Phase-contrast; (*b,e,h,* and *k*) Sm; (*c,f,i,* and *l*) CRLM. Arrow, chromosomes; arrowheads in *b,e,h,* and *k* show Sm immunoreactivity; arrowheads in *c,f,i,* and *l* show CRLM immunoreactivity. ×1,000.

relative to p28, p107 is the last to leave the domain speckle in prophase and the first to reassemble as a discrete domain. These studies show that individual components of the interchromatin domains can have unique mitotic segregation properties.

Reactivating Chicken Erythrocyte Nuclei Acquire CRLM Immunoreactivity

Polyclonal antibodies to RNA polymerase I (45) and U1, U2, U4, U5 and U6 snRNP (55) have been used to show that reactivation of chicken erythrocyte nuclei in mouse L-cell cytoplasm involves an influx of these molecules. Since chromatin decondensation (1, 2, 22, 26, 29), matrix assembly (27), and transcriptional activation (1, 2, 22, 26, 29) occur during erythrocyte nuclear reactivation, we examined reactivating nuclei for the occurrence of p107-containing interchromatin domains.

Chicken erythrocyte nuclei lacked CRLM immunoreactivity (Fig. 7, *g* and *h*), and did not show CRLM speckling when initially present in mouse L-cell cytoplasm. 16 h after fusion, heterokaryons (hybrids with both L-cell and erythrocyte nuclei) had mostly acquired CRLM immunoreactivity (Fig. 7, *a* and *b*), whereas in cybrids (hybrids lacking L-cell nuclei), only ~25% of the erythrocyte nuclei acquired CRLM reactivity (Fig. 7, *c–f*). Similar nuclear reactivation has been reported by Woodcock et al. (55) using both Sm and RNP antibodies in heterokaryons. However, in contrast to the results presented here, these authors observed an equal RNP nuclear reactivation in cybrids and heterokaryons. Our findings therefore suggest that the accumulation of p107 during nuclear reactivation depends largely on events controlled by the host nucleus. In this regard, the occurrence of "p107-reactivated" erythrocyte nuclei in only 25% of the cybrids suggests that p107 or its mRNA was present in the cytoplasm after these cells were enucleated. Cell cycle–dependent nuclear reactiva-

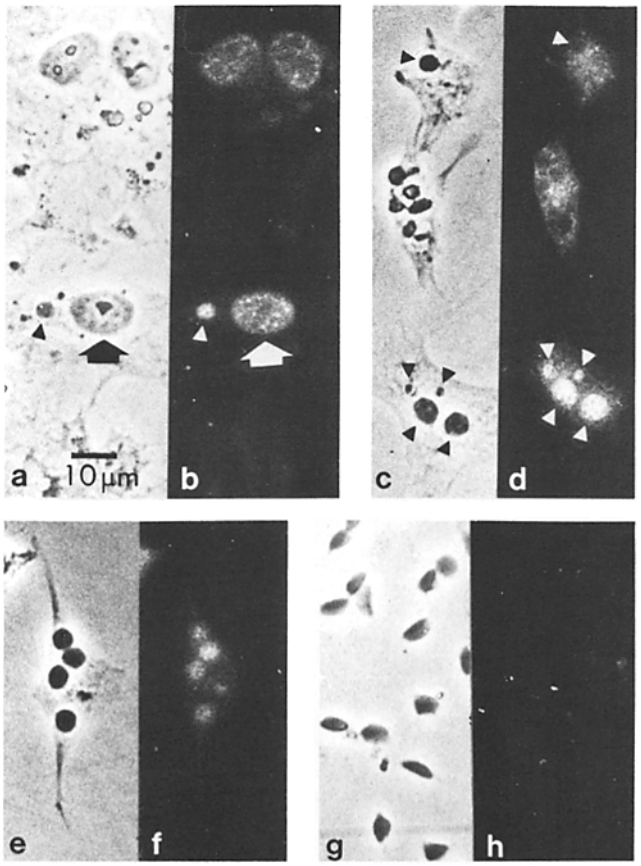

FIGURE 7 Binding of CRLM to mouse L-cells and reactivating chicken erythrocyte nuclei. (a and *b*) A heterokaryon that contains one L-cell nucleus (large arrow) and one reactivating chick erythrocyte nucleus (small arrowhead). Both show CRLM binding. Two other L-cell nuclei appear at the top of the micrograph. (*c–f*) Fusions between L-cell cytoplasts and chick erythrocyte nuclei (cybrids). The lower cybrid in *c* and *d* contains four erythrocyte nuclei (arrowheads), two of which show the enlargement characteristic of reactivation, while the other two remain pycnotic. All four show strong CRLM binding. In contrast, the two upper cybrids contain reactivating nuclei that do not bind CRLM. Another case of CRLM binding to cybrid nuclei is shown in *e* and *f*. (*g* and *h*) Unreactivated erythrocyte nuclei fail to bind CRLM in parallel experiments. The erythrocyte nuclei were somewhat swollen during the preparation in this instance. ×400.

tion events have been previously reported (29). Our data suggest, therefore, that the "p107-reactivation" competent cytoplasts might have been in late mitosis at the time of their enucleation.

DISCUSSION

Using biochemical and immunological techniques, we have identified an interchromatin 107-kD protein, p107, which is associated with the rat liver nuclear matrix via high salt- and DNase I-resistant interactions (47, 49).[2] The association of p107 with the matrix depends on the presence of undegraded RNA- and EDTA-chelatable divalent cations (47, 49).[2]

In this paper, we have studied the in situ localization of components of the high salt-resistant ribonucleoprotein network using monoclonal antibodies to the Sm antigen, p28, and polyclonal antibodies to p107. We show that in HeLa cells, PtK-2 cells, and Novikoff hepatoma cells, a portion of the total nuclear p28 (a component of U1, U2, U4, U5, and U6 snRNPs) co-localizes with p107 in discrete domains that are 1–1.5 μm in diameter. The remainder of p28 appears homogeneously distributed throughout the nucleoplasm. Though the nuclei of *Xenopus* kidney cells contained p28, p107 could not be detected. As both rat kidney cryosections (Smith, H. C., unpublished observation) and rat kangaroo kidney cells contained p107, the lack of p107 immunoreactivity in *Xenopus* kidney cells suggests evolutionary distinction in the occurrence of p107 or at least in the epitope that CRLM recognizes. Similarly, differences in immunoreactivity of the lamin proteins of the nuclear matrix have been observed when comparing *Xenopus* to other cell types (25).

Immunoelectron microscopy with CRLM showed that the peroxidase reaction product was confined to interchromatin domains and had an apparent fine structure that consisted of interconnected granules. The Sm antigen was concentrated in these domains, but also showed some general nucleoplasmic distribution.

Recent experiments have also shown that in addition to p28 and p107, interchromatin domains contain other U1 and U2 snRNP antigens (48) and a major liver protein, BA (see references 9 and 49). It is reasonable to presume, therefore, that additional components of the domains might be RNP proteins with similar speckled nuclear fluorescence (12, 24) along with hnRNA and selected U-snRNAs. Though several high molecular weight proteins (4, 19, 20, 23, 40, 52), hnRNA (11, 19–21, 23, 31, 32, 34, 35, 44, 52, 53), and the U1, U2, U4, U5, and U6 snRNAs (11, 32, 36) have been shown to be high salt-resistant components of the interchromatin domains, other components, such as BA, may be sensitive to high salt extraction. Taken together with the proposal that the interchromatin regions are the sites for hnRNA packaging, maturation, and transport to the cytoplasm (4, 19–22, 48, 49), our data suggest the possibility that many of these events may occur within the discrete domains (speckles) common to p28 and p107.

The importance of these domains was further suggested when p107 was observed to assemble within reactivating chicken erythrocyte nuclei. Nuclear swelling, chromatin decondensation, acquisition of a nuclear matrix structure, and an influx of stored macromolecules related to the synthesis, packaging, and metabolism of RNA have all been shown to be part of the nuclear reactivation process (1, 22, 26–29); thus, the presence of p107 within newly forming interchromatin domains may indicate a function for p107 in these processes. The immunocytochemical experiments presented above, taken together with the RNase sensitivity of the domains (47, 49)[2] suggest that one function of p107 in the domains might be to bind and package nascent RNA transcripts. This possibility is supported by our recent observation that the simultaneous inhibition of RNA polymerases I and II by 5, 6-dichloro-1-β-D-ribofuranosylbenzimidazole induced conformational changes in the interchromatin domains similar to those seen in the early and late stages of mitosis (47, 48, and unpublished observation). In this regard, the extranuclear assembly of p107 during mitosis suggest that while nascent transcripts might be involved in nuclear domain morphology, they probably are not solely responsible for domain assembly. An examination of the extranuclear complexes that contain p107 during mitosis may provide important information on the structural interactions. An understanding of why components of the interchromatin domains such as p28 have mitotic segregation properties so different

from p107 will also assist in further characterization of the structural and functional interactions within the domains. At this time it is unclear whether the extranuclear p107 domains translocate directly into daughter nuclei as macromolecular assemblies as has been described for other proteins (10, 14, 30, 33, 56).

In conclusion, we have presented experiments which show that the morphology of intranuclear domains that contain p107 and U-snRNPs is dependent on the condensation state and/or transcriptional activity of chromatin. Assembly of p107-containing domains during mitosis is an extranuclear process and co-localization of these domains with U-snRNPs in the daughter nuclei occurs only after chromatin decondensation in late telophase. Future biochemical and cytological analyses of other nuclear matrix–associated domains should provide an understanding of the assembly of the nuclear matrix itself.

The authors wish to thank Dr. Harris Busch for support and facilities; Linda A. Baldwin for expert technical assistance; and P. A. Dodson, L. D. Thompson, and L. M. Whiteman for excellent typographical assistance.

These studies were supported by a Cancer Research Center Grant CA-10893, P5 awarded to D. L. Spector from the National Cancer Institute, Department of Health and Human Services Public Health Service, and by the National Institutes of Health grant GM 32147 to C. L. F. Woodcock.

REFERENCES

1. Appels, R., L. Bolund, and N. R. Ringertz. 1974. Biochemical analysis of reactivated chick erythrocyte nuclei isolated from chick/HeLa heterokaryons. *J. Mol. Biol.* 87:339–355.
2. Appels, R., and N. R. Ringertz. 1975. Chemical and structural changes within chick erythrocyte nuclei introduced into mammalian cells by fusion. *Curr. Top. Dev. Biol.* 9:137–166.
3. Bachellerie, J. P., E. Puvion, and J. P. Zalta. 1975. Ultrastructural organization and biochemical characterization of chromatin RNA-protein complexes isolated from mammalian cell nuclei. *Eur. J. Biochem.* 58:327–337.
4. Berezney, R. 1980. Fractionation of the nuclear matrix. I. Partial separation into matrix protein fibrils and a residual ribonucleoprotein fraction. *J. Cell Biol.* 85:641–650.
5. Berezney, R. 1984. Organization and functions of the nuclear matrix. *In* Chromosomal Nonhistone Proteins Structural Associations. L. S. Hnilica, editor. CRC Press, Inc. Boca Raton, Florida. Vol. 4. 120–180.
6. Berezney, R., and D. S. Coffey. 1976. The nuclear protein matrix: isolation, structure, and functions. *Adv. Enzyme Regul.* 14:63–100.
7. Bernhard, W. 1969. A new staining procedure for electron microscopical cytology. *J. Ultrastruct. Res.* 27:250–265.
8. Bhorjee, J. S., S. L. Barclay, A. Wedrychowski, and A. M. Smith. 1983. Monoclonal antibodies specific for tight-binding human chromatin antigens reveal structural rearrangements within the nucleus during the cell cycle. *J. Cell Biol.* 97:389–396.
9. Catino, J. J., L. C. Yeoman, M. Mandel, and H. Busch. 1978. Characterization of a DNA binding protein from rat liver chromatin which decreases during growth. *Biochemistry.* 17:983–987.
10. Cepko, C. L., and P. A. Sharp. 1982. Assembly of adenovirus major capsid protein is mediated by a nonvirion protein. *Cell.* 31:407–415.
11. Ciejek, E. M., J. L. Nordstrom, M.-J. Tsai, and B. W. O'Malley. 1982. Ribonucleic acid precursors are associated with chick oviduct nuclear matrix. *Biochemistry.* 21:4945–4953.
12. Clevenger, C. V., and A. L. Epstein. 1984. Identification of a nuclear protein component of interchromatin granules using a monoclonal antibody and immunogold electron microscopy. *Exp. Cell Res.* 151:194–207.
13. Daskal, Y. 1981. Perichromatin Granules. *In* The Cell Nucleus. H. Busch, editor. Academic Press, Inc., New York. VIII:117–137.
14. DeRobertis, E. M., S. Lienhard, and R. F. Parisot. 1982. Intracellular transport of microinjected 5S and small nuclear RNAs. *Nature (Lond.).* 295:572–577.
15. Fakan, S. 1978. High resolution autoradiography studies on chromatin functions. *In* The Cell Nucleus. H. Busch, ed Academic Press, Inc. New York. V:3–53.
16. Fakan, S., and W. Bernhard. 1973. Nuclear labeling after prolonged ^{3}H-uridine incorporation as visualized by high resolution autoradiography. *Exp. Cell Res.* 79:431–444.
17. Fakan, S., and P. Nobis. 1978. Ultrastructural localization of transcription sites and of RNA distribution during the cell cycle of synchronized CHO cells. *Exp. Cell Res.* 113:327–337.
18. Fakan, S., E. Puvion, and G. Spohr. 1976. Localization and characterization of newly synthesized nuclear RNA in isolated rat hepatocytes. *Exp. Cell Res.* 99:155–164.
19. Fuchs, J.-P., and M. Jacob. 1979. Fractionation of constituents of ribonucleoprotein containing heterogeneous nuclear ribonucleic acid. *Biochemistry.* 18:4202–4208.
20. Gallinaro, H., E. Puvion, L. Kister, and M. Jacob. 1983. Nuclear matrix and hnRNP share a common structural constituent associated with premessenger RNA. *EMBO (Eur. Mol. Biol. Organ.) J.* 2:953–960.
21. Herman, R., L. Weymouth, and S. Penman. 1978. Heterogeneous nuclear RNA-protein fibers in chromatin-depleted nuclei. *J. Cell Biol.* 78:663–674.
22. Hernandez-Verdun, D., and M. Bouteille. 1979. Nucleologenesis in chick erythrocyte nuclei reactivated by cell fusion. *J. Ultrastruct. Res.* 69:164–179.
23. Jacob, M., G. Devillers, J. P. Fuchs, H. Gallinaro, R. Gattoni, C. Judes, and J. Stevenin. 1981. Isolation and structure of the ribonucleoprotein fibrils containing heterogeneous nuclear RNA. *In* The Cell Nucleus. H. Busch, editor. Academic Press, Inc., New York VIII:193–246.
24. Jones, R. E., C. S. Okamura, and T. E. Martin. 1980. Immunofluorescent localization of the proteins of nuclear ribonucleoprotein complexes. *J. Cell Biol.* 86:235–243.
25. Krohne, G., E. Debus, M. Osborn, K. Weber, and W. W. Franke. 1984. A monoclonal antibody against nuclear lamina proteins reveals cell type specificity in *Xenopus laevis*. *Exp. Cell Res.* 150:47–59.
26. Ladda, R. L., and R. D. Estensen. 1970. Introduction of a Heterogeneous Nucleus into Enucleated Cytoplasms of Cultured Mouse L-Cells. *Proc. Natl. Acad. Sci. USA.* 67:1528–1533.
27. LaFond, R. E., H. Woodcock, C. L. F. Woodcock, E. R. Kundahl, and J. J. Lucas. 1983. Generation of an internal matrix in mature avain erythrocyte nuclei during reactivation in cytoplasts. *J. Cell Biol.* 96:1815–1819.
28. Lerner, E. A., M. R. Lerner, C. A. Janeway, and J. A. Steitz. 1981. Monoclonal antibodies to nucleic acid–containing cellular constituents: probes for molecular biology and autoimmune disease. *Proc. Natl. Acad. Sci. USA.* 78:2737–2741.
29. Lipsich, L. A., J. J. Lucas, and J. R. Kates. 1978. Cell cycle dependence of the reactivation of chick erythrocyte nuclei after transplantation into mouse L-929 cell cytoplasts. *J. Cell Physiol.* 97:199–208.
30. Lohka, M. J., and Y. Masui. 1984. Roles of cytosol and cytoplasmic particles in nuclear envelope assembly and sperm pronuclear formation in cell-free preparations from amphibian eggs. *J. Cell Biol.* 98:1222–1230.
31. Long, B. H., C.-Y. Huang, and A. O. Pogo. 1979. Isolation and characterization of the nuclear matrix in Friend erythroleukemia cells: chromatin and hnRNA interations with the nuclear matrix. *Cell.* 18:1079–1090.
32. Long, B. H., and R. L. Ochs. 1983. Nuclear matrix hnRNA, and snRNA in Friend erythroleukemia nuclei depleted of chromatin by low ionic strength EDTA. *Biol. Cell.* 48:89–98.
33. Madore, S. J., E. D. Wieben, G. R. Kunkel, and T. Pederson. 1984. Precursors of U4 Small Nuclear RNA. *J. Cell Biol.* 99:1140–1144.
34. Maundrell, K., E. S. Maxwell, E. Puvion, and K. Scherrer. 1981. The nuclear matrix of duck erythroblasts is associated with Globen mRNA coding sequences but not with the major proteins of 40S nuclear RNP. *Exp. Cell Res.* 136:435–445.
35. Miller, T. E., C.-Y. Huang, and A. O. Pogo. 1978. Rat liver nuclear skeleton and ribonucleoprotein complexes containing hnRNA. *J. Cell Biol.* 76:675–691.
36. Miller, T. E., C.-Y. Huang, and A. D. Pogo. 1978. Rat liver nuclear skeleton and small molecular weight RNA species. *J. Cell Biol.* 76:692–704.
37. Muller, M., E. Spiess, and D. Werner. 1983. Fragmentation of the nuclear matrix on a mica target. *Eur. J. Cell Biol.* 31:158–166.
38. Nakayasu, H., H. Mori, and K. Ueda. 1982. Association of small nuclear RNA-protein complex with the nuclear matrix from bovine lymphocytes. *Cell Struct. Funct.* 7:253–262.
39. Nash, R. E., E. Puvion, and W. Bernhard. 1975. Perichromatin fibrils as components of rapidly labeled extranucleolar RNA. *J. Ultrastruct. Res.* 53:395–405.
40. Northemann, W., H. Seifert, and P. C. Heinrich. 1979. The effect of sodium chloride on the structure of ribonucleoprotein particles from rat liver nuclei. *Hoppe-Seyler's Z. Physiol. Chem.* 360:877–888.
41. Puvion, E., and W. Bernhard. 1975. Ribonucleoprotein components of liver cell nuclei as visualized by cryoultramicrotomy. *J. Cell Biol.* 67:200–214.
42. Puvion, E., and M. Lange. 1980. Functional significance of perichromatin granule accumulation induced by cadmium chloride in isolated rat liver cells. *Exp. Cell Res.* 128:47–58.
43. Puvion, E., and G. Moyne. 1978. Intranuclear migration of newly synthesized extranucleolar ribonucleoproteins. *Exp. Cell Res.* 115:79–88.
44. Ross, D. A., R. W. Yen, and C.-B. Chae. 1982. Association of globin ribonucleic acid and its precursors with the chicken erythroblast nuclear matrix. *Biochemistry.* 21:764–771.
45. Scheer, U., G. Lanfranchi, K. M. Rose, W. W. Franke, and N. R. Ringertz. 1983. Migration of rat RNA polymerase I into chick erythrocyte nuclei undergoing reactivation in chick-rat heterokaryons. *J. Cell Biol.* 97:1641–1643.
46. Smith, H. C., and R. Berezney. 1980. DNA polymerase α is tightly bound to the nuclear matrix of actively replicating liver. *Biochem. Biophys. Res. Commun.* 97:1541–1547.
47. Smith, H. C., D. L. Spector, and H. Busch. 1984. Identification of a 107-kD Protein which is associated with the nuclear matrix via RNase/EDTA sensitive interactions. *J. Cell Biol.* 99(4, Pt. 2):129a. (*Abstr*)
48. Spector, D. L. 1984. Colocalization of U1 and U2 small nuclear RNPs by immunocytochemistry. *Biol. Cell.* 51:109–112.
49. Spector, D. L., R. L. Ochs, H. C. Smith, F. C. Bennett, and L. C. Yeoman. 1984. Antibody probes to nuclear domains. I. Partial characterization of nuclear protein clusters (NPC's). *J. Cell Biol.* 99 (4, Pt. 2):130a (*Abstr*)
50. Spector, D. L., W. H. Schrier, and H. Busch. 1983. Immunoelectron microscopic localization of snRNPs. *Biol. Cell.* 49:1–10.
51. Steele, W. J., and H. Busch. 1966. Studies on the ribonucleic acid components of the nuclear ribonucleoprotein network. *Biochem. Biophys. Acta.* 129:54–67.
52. Stevenin, J., and M. Jacob. 1974. Effects of sodium chloride and pancreatic ribonuclease on the rat-brain nuclear particles: the fate of the protein moiety. *Eur. J. Biochem.* 47:129–137.
53. van Eekelen, C. A. G., and W. J. van Venrooji. 1981. HnRNA and its attachment to a nuclear protein matrix. *J. Cell Biol.* 88:554–563.
54. Vogelstein, B., and B. F. Hunt. 1982. A subset of small nuclear ribonucleoprotein particle antigens is a component of the nuclear matrix. *Biochem. Biophys. Res. Commun.* 105:1224–1232.
55. Woodcock, C. L. F., R. E. LaFond, H. Woodcock, L. A. Baldwin, and J. S. Bhorjee. 1984. Reactivation of avian erythrocyte nuclei in mammalian cytoplasts: a dominant role for pre-existing cytoplasmic components. *Exp. Cell Res.* 154:155–170.
56. Zeller, R., T. Nyffenegger, and E. M. DeRobertis. 1983. Nucleocytoplasmic distribution of snRNPs and stockpiled snRNA-binding proteins during oogenesis and early development in *Xenopus laevis*. *Cell.* 32:425–434.